Inorg. Chem. **2004**, *43*, 7170–7179

Copper(II) Complexes with Substituted Thiosemicarbazones of α-Ketoglutaric Acid: Synthesis, X-ray Structures, DNA Binding Studies, and Nuclease and Biological Activity

Monica Baldini,[†] Marisa Belicchi-Ferrari,*[,†] Franco Bisceglie,[†] Pier Paolo Dall'Aglio,[‡] Giorgio Pelosi,[†] Silvana Pinelli,[‡] and Pieralberto Tarasconi[†]

Dipartimento di Chimica Generale ed Inorganica, Chimica Analitica, Chimica Fisica, and Dipartimento di Clinica Medica, Nefrologia e Scienza della Prevenzione, Università degli Studi di Parma, 43100 Parma, Italy

Received January 28, 2004

New α-ketoglutaric acid thiosemicarbazone (H_3ct) derivatives and their copper complexes were synthesized and characterized by analytical and spectroscopic (IR and NMR) methods. For two of the ligands, Me-H_3ct and Allyl-H_3ct, and for a complex, $[Cu(Me\text{-}Hct)(OH_2)]_n \cdot 2nH_2O$, the X-ray structures were also determined. In the latter the copper atom shows a 4 + 1 pyramidal coordination, a water oxygen appears in the apical position, and three of the basal positions are occupied by the SNO tridentate ligand and the fourth by a carboxylic oxygen of an adjacent molecule that gives rise to a polymeric chain. DNA binding constants were determined, and studies of thermal denaturation profiles and nuclease activity were also performed. Tests in vitro on human leukemia cell line U937 were carried out on cell growth inhibition, cell cycle, and apoptosis induction.

Introduction

Thiosemicarbazones and their derivatives have raised considerable interest in chemistry, pharmacology, and biology thanks to their antibacterial, antiviral, and antitumor activity.[1−9] In particular our previous studies revealed that copper complexes with aromatic thiosemicarbazones (pyridoxal,[10,11] 5-formyluracil[12−14]) affect the complicated mechanisms that lead to a leukemic transformation by inhibiting replication and by triggering apoptotic processes and thus they act as potentially important antitumor substances. The debate on the lability of coordinate bonds to copper(II) is well-known in the community of bioinorganic chemists especially as regards copper-based drugs. Nevertheless the formation constants of these thiosemicarbazones complexes[15,16] are large enough to render most of the molecules that can be found in a culture medium ineffective in competing for complexation. This phenomenon is therefore much limited in the case of SNO chelate systems such as

* Author to whom correspondence should be addressed. E-mail: marisa.ferrari@unipr.it. Tel.: +39-0521-905-420. Fax: +39-0521-905-557.

[†] Dipartimento di Chimica Generale ed Inorganica, Chimica Analitica, Chimica Fisica.

[‡] Dipartimento di Clinica Medica, Nefrologia e Scienza della Prevenzione.

(1) Afrasiabi, Z.; Sinn, E.; Padhye, S.; Dutta, S.; Padhye, S.; Newton, C.; Anson, C. E.; Powell, A. K. *J. Inorg. Biochem.* **2003**, *95*, 306−314.
(2) Byrnes, R. W.; Mohan, M.; Antholine, W. E.; Xu, R. X.; Petering, D. H. *Biochemistry* **1990**, *29*, 7046−7053.
(3) Kolocouris, A.; Dimas, K.; Pannecouque, C.; Witvrouw, M.; Foscolos, G.-B.; Stamatiou, G.; Fytas, G.; Zoidis, G.; Kolocouris, N.; Andrei, G.; Snoeck, R.; De Clercq, E. *Bioorg. Med. Chem.* **2002**, *12*, 723−727.
(4) Hall, I. H.; Chen, S. Y.; Barners, B. J.; West, D. X. *Met.-Based Drugs* **1999**, *6*, 143−147.
(5) Kelly, P. F.; Slawin, A. M. Z.; Soriano-Rama, A. *J. Chem. Soc., Dalton Trans.* **1996**, 53−60.
(6) Klayman, D. L.; Bartosovich, J. F.; Griffin, T. S.; Mason, C. J.; Scovill, J. P. *J. Med. Chem.* **1979**, *22*, 855−862.
(7) Bermejo, E.; Carballo, R.; Castineiras, A.; Dominguez, R.; Liberta, A. E.; Maichle-Mossmer, C.; West, D. X. *Z. Naturforsch.* **1999**, *B54*, 777−787.
(8) Lakovidou, Z.; Papageorgiou, A.; Demertzis, M. A.; Mioglou, E.; Mourelatos, D.; Kotsis, A.; Yadav, P. N.; Kovala-Demertzi, D. *Anticancer Drugs* **2001**, *12*, 65−70.
(9) Condit, R. C.; Easterly, R.; Pacha, R. F.; Fathi, Z.; Meis, R. J. *Virology* **1991**, *185*, 857−861.
(10) Belicchi Ferrari, M.; Gasparri Fava, G.; Tarasconi, P.; Albertini, R.; Pinelli, S.; Starcich, R. *J. Inorg. Biochem.* **1994**, *53*, 13−25.
(11) Belicchi Ferrari, M.; Bisceglie, F.; Leporati, E.; Pelosi, G.; Tarasconi, P.; Pinelli, S. *Bull. Chem. Soc. Jpn.* **2002**, *75*, 781−788.
(12) Belicchi Ferrari, M.; Gasparri Fava, G.; Leporati, E.; Pelosi, G.; Rossi, R.; Tarasconi, P.; Albertini, R.; Bonati, A.; Lunghi, P.; Pinelli, S. *J. Inorg. Biochem.* **1998**, *70*, 145−154.
(13) Belicchi Ferrari, M.; Bisceglie, F.; Pelosi, G.; Tarasconi, P.; Albertini, R.; Bonati, A.; Lunghi, P.; Pinelli, S. *J. Inorg. Biochem.* **2001**, *83*, 169−179.
(14) Baldini, M.; Belicchi-Ferrari, M.; Bisceglie, F.; Pelosi, G.; Pinelli, S.; Tarasconi, P. *Inorg. Chem.* **2003**, *42*, 2049−2055.
(15) Borges, R. H. U.; Oaniago, E.; Beraldo, H. *J. Inorg. Biochem.* **1997**, *65*, 267−275.
(16) Offiong, O. *Transition Met. Chem.* **1998**, *23*, 553−555.

10.1021/ic049883b CCC: $27.50
Published on Web 10/05/2004

Chart 1

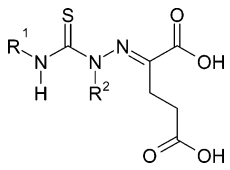

these with thiosemicarbazones. Given the order of magnitude of the formation constants, Cu−thiosemicarbazone species can be assumed present at high percentage even in the presence of strong competitors, whereas Cu−Cl, Cu−OH_2, and Cu−O(OOCR) bonds quickly dissociate and allow bonding formation with other ligands (for instance biomolecules). We focused then our attention on aliphatic thiosemicarbazones derived from natural aldehydes (which are potentially SN bidentate) and their nickel and copper complexes.[17] More recently our attention was devoted to copper complexes of the α-ketoglutaric acid thiosemicarbazone (H_3ct), an aliphatic ligand with many potential donor atoms and a variety of possible conformations which determine a versatile chelating behavior. In particular, coordination geometry, ligand behavior, and biological activity were compared for two copper complexes $[Cu(H_2ct)Cl]_n[\{Cu(H_2ct)Cl\}_2]$ and $[Cu(Hct)]_n \cdot 3nH_2O$ which exert proliferation inhibition through an apoptosis mechanism on cell line U937.[18] To extend further our knowledge of the chemical and biological behavior of α-ketoglutaric acid thiosemicarbazones and to widen our comprehension of the mechanism of action and of the possible biological targets, we synthesized condensation compounds of the α-ketoglutaric acid with seven N-substituted thiosemicarbazides possessing aliphatic and aromatic groups (see Chart 1) that were subsequently used for preparing copper complexes. The choice on the substituents was made to find out which part of the molecule is determinant in endowing the complex of activity and also in the light of the considerations reported by Hambley and co-workers[19] that the stability of copper−thiosemicarbazone species is increased in the case the external surface of the complex molecule is hydrophobic.

Ligands Me-H_3ct (**1**) and Allyl-H_3ct (**3**) and complex $[Cu(Me\text{-}Hct)(OH_2)]_n \cdot 2nH_2O$ (**9**) were also characterized by X-ray diffractometry. With the aim to ascertain the entity and the mode of interaction that active molecules exert toward specific biological targets, the binding interactions of the new synthesized complexes with calf thymus DNA were investigated by absorption titration in the UV−visible region and thermal denaturation (melting temperature). Nuclease activity study was also performed to verify if oxidative breakings take place. To confirm the cytotoxicity of this class of compounds, tests in vitro (cell proliferation inhibition and apoptosis induction) on human leukemia cell line U937 were performed, together with a study of their cell cycle.

Experimental Section

Physical Measurements. Elemental analyses (C, H, N, S) were performed with a Carlo Erba model EA 1108 automatic analyzer. IR spectra (4000−400 cm^{-1}) for KBr disks were recorded on a Nicolet 5PC FT. Chemical ionization-mass (*m*/*z*, 70 eV) fragmentation patterns were obtained, using samples dissolved in methanol, with a Finnegan 1020 6c mass spectrometer equipped with a quadrupole mass selector MATSSQ 710. Melting points were determined with a Gallenkamp instrument. UV measurements were performed on a Perkin-Elmer UV/vis Lambda 25 spectrometer with quartz cuvettes. ^{1}H NMR spectra were obtained at room temperature with a Brucker AMX-300 MHz spectrometer, and chemical shifts are given in units of δ relative to TMS as an internal reference, using CD_3OD as the solvent.

Materials. 4-Methyl-3-thiosemicarbazide, 97% (Aldrich), 4-ethyl-3-thiosemicarbazide, 97% (Aldrich), 4-allyl-3-thiosemicarbazide, 97% (Aldrich), 2-methyl-3-thiosemicarbazide, 97% (Aldrich), 2,4-dimethyl-3-thiosemicarbazide, 98% (Lancaster), 4-phenyl-3-thiosemicarbazide, 99% (Janssen), 4-(3-methylphenyl)-3-thiosemicarbazide, 97% (Aldrich), and $CuCl_2 \cdot 2H_2O$ (Carlo Erba) were commercially available and used without further purification. Calf thymus (CT) DNA was obtained from Serva and used as received. TRIS and TRIS-acetate-EDTA 10× buffers and agarose were purchased from Sigma. pBR322 DNA plasmid (Roche), DirectLoad Wide-Range DNA marker, ethidium bromide, and gel loading solution type I 6× concentrate were from Sigma.

Preparation of the Ligands. The general procedure used to prepare the ligands can be summarized as follows: to a solution (the solvent differs from case to case depending on the substance and is reported below) of substituted thiosemicarbazide, obtained by magnetic stirring and slight heating, an equimolar amount of α-ketoglutaric acid, dissolved in the same solvent, is added dropwise. After a while, a white powder is formed, isolated by filtration, and analyzed. The purity of the products dissolved in the minimum quantity of CH_3OH was checked by TLC analysis using 1:1 (v/v) THF/acetone as eluting mixture and revealed by means of a UV lamp at 254 nm showing the spots of the pure products. Purity was also confirmed by the melting points. Ligands were recrystallized from CH_3OH solutions, obtained as crystals, and two of them were characterized by X-ray analysis. Crystalline products presented the same analytical details of the powders. The reaction is reported in Scheme 1.

Synthesis of Me-H_3ct (1) (R^1 = Me, R^2 = H). A 0.26 g (2.5 mmol) amount of 4-methyl-3-thiosemicarbazide was solubilized in 10 mL of H_2O. An equimolar amount (0.36 g) of α-ketoglutaric acid was dissolved in 7 mL of H_2O, added dropwise to the solution of the thiosemicarbazide, and stirred for 30 min. Anal. Calcd for $C_7H_{11}N_3O_4S$: C, 36.01; H, 4.28; N, 18.00; S, 13.72. Found: C, 35.42; H, 4.85; N, 17.82; S, 14.42. IR (KBr disks, cm^{-1}): 3581 (w) ν(OH); 3337 (s) and 3191 (m) ν(NH); 2946 (w) and 2916 (w) ν(CH); 1718 (s) and 1700 (s) ν(C═O); 1600 (w) and 1560 (m) ν(C═N); 869 (w) ν(C═S). UV−visible (solvent MeOH, nm): 206 ($n \rightarrow \sigma^*$); 256 and 307 ($n \rightarrow \pi^*$). ^{1}H NMR (CD_3OD, ppm): 2.65(m) $-CH_2CH_2COOH$; 2.87(m) $-CH_2CH_2COOH$; 3.16 (d) of methyl substituent; 8.40 (d) NH aminic; 10.75 (d) NH hydrazinic. Mass spectrum (*m*/*z*): 262 (M^+ + Et); 234 (MH^+); 215 ($M^+ - H_2O$); 188 ($MH^+ - CO_2$ or M^+ − COOH). Mp: 174 °C. Yield = 72%.

Synthesis of Et-H_3ct·H_2O (2) (R^1 = Et, R^2 = H). A 0.3 g (2.5 mmol) amount of 4-ethyl-3-thiosemicarbazide was solubilized in

(17) Belicchi Ferrari, M.; Bisceglie, F.; Pelosi, G.; Sassi, M.; Tarasconi, P.; Cornia, M.; Capacchi, S.; Albertini, R.; Pinelli, S. *J. Inorg. Biochem.* **2002**, *90*, 113−126.
(18) Belicchi Ferrari, M.; Bisceglie, F.; Gasparri-Fava, G.; Pelosi, G.; Tarasconi, P.; Albertini, R.; Pinelli, S. *J. Inorg. Biochem.* **2002**, *89*, 36−44.
(19) Weder, J. E.; Dillon, C. T.; Hambley, T. W.; Kennedy, B. J.; Lay, P. A.; Biffin, J. R.; Regtop, H. L.; Davies, N. M. *Coord. Chem. Rev.* **2002**, *232*, 95−126.

Scheme 1

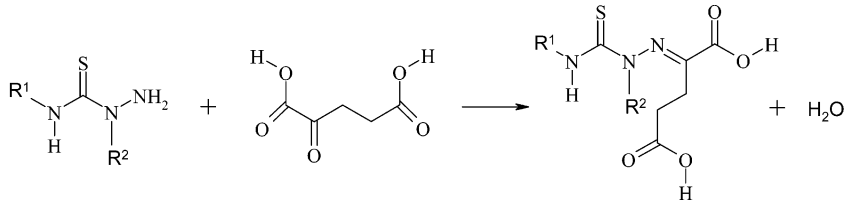

10 mL of H_2O. An equimolar amount (0.36 g) of α-ketoglutaric acid was dissolved in 7 mL of H_2O, added dropwise to the solution of the thiosemicarbazide, and stirred for 30 min. Anal. Calcd for $C_8H_{15}N_3O_5S$: C, 36.18; H, 5.65; N, 15.83; S, 12.06. Found: C, 36.57; H, 5.69; N, 15.56; S, 12.65. IR (KBr disks, cm^{-1}): 3436 (m) ν(OH); 3350 (w) and 3236 (w) ν(NH); 2976 (w) and 2936 (w) ν(CH); 1709 (s) ν(C═O); 1543 (m) ν(C═N); 836 (w) ν(C═S). UV−visible (solvent MeOH, nm): 228 ($\pi \rightarrow \pi^*$); 272 ($n \rightarrow \pi^*$). ^{1}H NMR (CD_3OD, ppm): 1.24 (t) CH_3 of substituent; 2.65 (m) CH_2CH$_2$COOH; 2.87 (m) −CH$_2$CH_2COOH; 3.70 (m) CH_2 of substituent; 8.42 (d) NH aminic; 10.77 (d) NH hydrazinic. Mass spectrum (*m*/*z*): 276 (M^+ + Et); 248 (MH^+); 230 ($MH^+ - H_2O$); 212 ($MH^+ - H_2S$); 202 ($MH^+ - CO_2$ or $M^+ -$ COOH). Mp: 157 °C. Yield = 73%.

Synthesis of Allyl-H$_3$ct (3) (R^1 = Allyl, R^2 = H). A 0.33 g (2.5 mmol) amount of 4-allyl-3-thiosemicarbazide was solubilized in 10 mL of H_2O. An equimolar amount (0.36 g) of α-ketoglutaric acid was dissolved in 7 mL of H_2O, added dropwise to the solution of the thiosemicarbazide, and stirred for 2 h. Anal. Calcd for $C_9H_{13}N_3O_4S$: C, 41.65; H, 5.01; N, 16.19; S, 12.34. Found: C, 41.89; H, 4.96; N, 15.92; S, 12.91. IR (KBr disks, cm^{-1}): 3361 (w) ν(OH); 3204 (m) ν(NH); 2924 (w) ν(CH); 1710 (s) and 1681 (s) ν(C═O); 1560 (m) ν(C═N); 907 (w) ν(C═S). UV−visible (solvent MeOH, nm): 288 ($n \rightarrow \pi^*$). ^{1}H NMR (CD_3OD, ppm): 1.24 (t) CH_3 of substituent; 2.64(m) −CH_2CH$_2$COOH; 2.86 (m) −CH$_2$CH_2COOH; 4.31 (m) CH$_2$═CHCH_2; 5.20 (m) CH_2═CHCH$_2$; 5.97 (m) CH$_2$═CHCH$_2$; 8.40 (d) NH aminic; 10.75 (d) NH hydrazinic. Mass spectrum (*m*/*z*): 274 (M^+ + Me); 260 (MH^+); 241 ($M^+ - H_2O$); 224 ($MH^+ - H_2S$); 214 ($MH^+ - CO_2$ or $M^+ -$ COOH). Mp: 172.5 °C. Yield = 41%.

Synthesis of 2-Me-H$_2$ct (4) (R^1 = H, R^2 = Me). A 0.15 g (1.4 mmol) amount of 2-methyl-3-thiosemicarbazide was solubilized in 10 mL of THF. An equimolar amount (0.2 g) of α-ketoglutaric acid was dissolved in 7 mL of THF, added dropwise to the solution of the thiosemicarbazide, and stirred for 2 h. Anal. Calcd for $C_7H_{11}N_3O_4S$: C, 36.01; H, 4.28; N, 18.00; S, 13.72. Found: C, 36.67; H, 4.66; N, 17.82; S, 13.99. IR (KBr disks, cm^{-1}): 3329 (w) ν(OH); 3156 (m) ν(NH); 3030 (w) ν(CH); 1740 (s) and 1676 (s) ν(C═O); 1613 (s) ν(C═N); 814 (w) ν(C═S). UV−visible (solvent MeOH, nm): 213 ($n \rightarrow \pi^*$). ^{1}H NMR (CD_3OD, ppm): 2.65 (m) −CH_2CH$_2$COOH; 2.87 (m) −CH$_2$CH_2COOH; 3.50 (s) of methyl hydrazinic; 8.42 (s) NH_2 aminic. Mass spectrum (*m*/*z*): 215 ($M^+ - H_2O$); 200 ($MH^+ - H_2S$). Mp: 164 °C. Yield = 76%.

Synthesis of 2,4-Me$_2$-H$_2$ct (5) (R^1 = Me, R^2 = Me). A 0.36 g (3 mmol) amount of 2,4-dimethyl-3-thiosemicarbazide was solubilized in 20 mL of MeOH. An equimolar amount (0.44 g) of α-ketoglutaric acid was dissolved in 10 mL of MeOH, added dropwise to the solution of the thiosemicarbazide, and stirred for 2 h. Anal. Calcd for $C_8H_{13}N_3O_4S$: C, 38.82; H, 5.25; N, 16.98; S, 12.94. Found: C, 39.51; H, 5.13; N, 16.74; S, 13.16. IR (KBr disks, cm^{-1}): 3162 (w) ν(OH); 3049 (m) and 2848 (w) ν(NH); 2839 (w) ν(CH); 1752 (s) and 1653 (s) ν(C═O); 747(w) ν(C═S). UV−visible (solvent MeOH, nm): 214 ($n \rightarrow \pi^*$). ^{1}H NMR (CD_3OD, ppm): 2.65 (m) −CH_2CH$_2$COOH; 2.87 (m) −CH$_2$CH_2COOH; 3.42 (s) of methyl aminic; 3.50 (s) of methyl hydrazinic; 8.45 (s) NH aminic. Mass spectrum (*m*/*z*): 229 ($M^+ - H_2O$); 212 ($MH^+ - H_2S$). Mp: 154.5 °C. Yield = 87%.

Synthesis of Ph-H$_3$ct (6) (R^1 = Ph, R^2 = H). A 0.66 g (4 mmol) amount of 4-phenyl-3-thiosemicarbazide was solubilized in 40 mL of EtOH. An equimolar amount (0.58 g) of α-ketoglutaric acid was dissolved in 20 mL of EtOH, added dropwise to the solution of the thiosemicarbazide, and stirred for 3 h. Anal. Calcd for $C_{12}H_{13}N_3O_4S$: C, 48.76; H, 4.40; N, 14.22; S, 10.83. Found: C, 48.98; H, 4.32; N, 14.02; S, 11.09. IR (KBr disks, cm^{-1}): 3285 (m) ν(NH); 3084 (w) ν(CH aromatic); 2990 (w) ν(CH aliphatic); 1698 (s) ν(C═O); 1595(s) ν(C═C aromatic); 1541 (s) ν(C═N); 1437 (m) δ(OH); 1296 (m) δ(CH aromatic); 1166 (m) ν(CN); 935 (m) and 747 (m) ν(C═S); 615 (m) fingerprint. UV−visible (solvent MeOH, nm): 304 ($\pi \rightarrow \pi^*$). ^{1}H NMR (CD_3OD, ppm): 2.65 (m) −CH_2CH$_2$COOH; 2.87 (m) −CH$_2$CH_2COOH; 7.70 (m) aromatic hydrogens; 8.43 (m) NH aminic; 10.75 (s) NH hydrazinic. Mass spectrum (*m*/*z*): 295 (M^+); 278 ($MH^+ - H_2O$); 260 ($MH^+ - H_2S$); 250 ($MH^+ - CO_2$ or $M^+ -$ COOH); 217 ($M^+ -$ Ph). Mp: 154 °C. Yield = 98%.

Synthesis of 3-Me-Ph-H$_3$ct (7) (R^1 = 3-Me-Ph, R^2 = H). A 0.18 g (1 mmol) amount of 4-(3-methylphenyl)-3-thiosemicarbazide was solubilized in 20 mL of MeOH. An equimolar amount (0.14 g) of α-ketoglutaric acid was dissolved in 10 mL of MeOH, added dropwise to the solution of the thiosemicarbazide, and stirred for 3 h. Anal. Calcd for $C_{13}H_{15}N_3O_4S$: C, 50.43; H, 4.85; N, 13.58; S, 10.34. Found: C, 50.25; H, 4.82; N, 13.35; S, 10.45. IR (KBr disks, cm^{-1}): 3326 (w) ν(OH); 3194 (w) ν(NH); 3019 (w) ν(CH aromatic); 2922 (w) ν(CH aliphatic); 1710 (s) and 1682(s) ν(C═O); 1537(s) ν(C═C aromatic); 1446 (m) δ(OH); 1276 (w) δ(CH aromatic); 1200 (m) ν(CN); 935 (m) and 789 (w) ν(C═S); 646 (w) fingerprint. UV−visible (solvent MeOH, nm): 206 ($n \rightarrow \sigma^*$); 305 ($\pi \rightarrow \pi^*$).^{1}H NMR (CD_3OD, ppm): 2.41 (s) CH_3Ar; 2.65 (m) −CH_2CH$_2$COOH; 2.87 (m) −CH$_2$CH_2COOH; 7.69 (m) aromatic hydrogens; 8.43 (m) NH aminic; 10.75 (s) NH hydrazinic. Mass spectrum (*m*/*z*): 338 (M^+ + Et); 309 (M^+); 292 ($MH^+ - H_2O$); 274 ($MH^+ - H_2S$); 264 ($MH^+ - CO_2$ or $M^+ -$ COOH). Mp: 161.5 °C. Yield = 91%.

Preparation of the Complexes. To a solution of the ligand (the solvent differs from case to case depending on the substance and is reported below), a solution containing an equimolar amount of $CuCl_2 \cdot 2H_2O$ dissolved in the same solvent is added dropwise. The resulting mixture is stirred for 1 h at room temperature. By slow evaporation of the solvent, a green or blue microcrystalline powder or crystals are formed. All compounds were recrystallized in several solvents as CH_3OH, C_2H_5OH, and THF. In all cases crystals were obtained, but only for **9** were crystals of size suitable for X-ray diffraction collected.

Only for obtaining complexes with the ligand Me-H$_3$ct (**1**) the pH was adjusted to 7 with NaOH before the addition of the metal salt solution.

Synthesis of [Cu(Me-H$_2$ct)Cl]·H$_2$O (8). A 0.32 g (1.4 mmol) amount of Me-H$_3$ct (**1**) was solubilized in 13 mL of H_2O. Before the addition of the metal salt solution, the pH value was adjusted

Table 1. Experimental Data for Crystallographic Analyses

	Me-H_3ct (**1**)	Allyl-H_3ct (**3**)	$[Cu(Me\text{-}Hct)(OH_2)]_n \cdot 2nH_2O$ (**9**)
formula	$C_{14}H_{24}N_6O_9S_2$	$C_9H_{13}N_3O_4S$	$C_7H_{15}CuN_3O_7S$
M_r	484.50	259.28	348.81
cryst system	monoclinic	monoclinic	triclinic
space group	$P2_1/n$	$P2_1/n$	$P\bar{1}$
a (Å)	16.209(3)	13.227(3)	8.993(1)
b (Å)	6.788(3)	5.269(3)	9.749(1)
c (Å)	20.634(3)	18.927(3)	8.919(1)
α (deg)	90.0	90.0	111.00(2)
β (deg)	111.80(2)	91.86(2)	118.68(2)
γ (deg)	90.0	90.0	71.49(2)
V (Å^3)	2108(1)	1318.4(4)	630.3(2)
λ (Å)	1.541 84	0.710 69	0.710 69
Z	4	4	2
D_c (Mg/m^3)	1.53	1.31	1.84
F(000)	1016	544	358
μ (cm^{-1})	28.44	2.53	1.93
cryst size (mm)	0.3 × 0.5 × 0.3	0.6 × 0.5 × 0.2	0.4 × 0.7 × 0.5
diffractometer	CAD4	Philips	Philips
θ min−max (deg)	3−50	3−30	3−30
dataset	−18/18, 0/7, 0/23	−18/18, 0/7, 0/26	−12/12, −12/12, 0/12
tot. reflcns, unique reflcns	3521, 3128	7690, 3847	3680, 3680
obsd reflcns [$I > 2.0\sigma(I)$]	2865	1044	2619
$N_{reflcns}$, N_{params}	3128, 368	1044, 177	3680, 179
R, wR2, S[a]	0.059, 0.16, 1.13	0.044, 0.14, 0.74	0.048, 0.14, 1.41

[a] $R = \Sigma||F_o| - |F_c||/\Sigma|F_o|$; $wR2 = \{\Sigma[w(F_o^2 - F_c^2)^2]/\Sigma w(F_o^2)^2]\}^{1/2}$; $S = \{\Sigma[w(F_o^2 - F_c^2)^2]/(n - p)\}^{1/2}$, where n = number of reflections and p = number of parameters refined.

to 7 with NaOH. An equimolar amount (0.25 g) of $CuCl_2 \cdot 2H_2O$ was then dissolved in 2 mL of H_2O, added to the ligand solution, and stirred for 1 h. Anal. Calcd for $C_7H_{12}N_3O_5SCuCl$: C, 24.05; H, 3.43; N, 12.03; S, 9.16. Found: C, 24.38; H, 3.36; N, 11.73; S, 9.05. IR (KBr disks, cm^{-1}): 3438 (m) H_2O of crystallization; 3219 (m) ν(NH); 2982 (m) and 2937 (w) ν(CH); 1718 (s) and 1635 (s) ν(C═O); 1600 (w) ν(C═N); 806 (w) ν(C═S). Mp: 193.5 °C.

Synthesis of $[Cu(Me\text{-}Hct)(OH_2)]_n \cdot 2nH_2O$ (9). A 0.32 g (1.4 mmol) amount of Me-H_3ct was dissolved in 13 mL of H_2O. Before the addition of the metal salt solution, the pH value was adjusted to 7 with NaOH. An equimolar amount (0.25 g) of $CuCl_2 \cdot 2H_2O$ was then dissolved in 2 mL of H_2O, added to the ligand solution, and stirred for 1 h. Anal. Calcd for $C_7H_{15}N_3O_7SCu$: C, 24.07; H, 4.31; N, 12.03; S, 9.17%. Found: C, 24.43; H, 3.98; N, 12.34; S, 9.41. IR (KBr disks, cm^{-1}): 3329 (s) ν(NH); 2982 (m) and 2937 (w) ν(CH); 1710 (s) and 1558 (s) ν(C═O); 1600 (w) ν(C═N); 806 (w) ν(C═S). Mp: 202 °C.

Synthesis of $[Cu(Et\text{-}H_2ct)Cl] \cdot H_2O$ (10). A 0.5 g (2 mmol) amount of Et-H_3ct·H_2O was dissolved in 50 mL of MeOH. An equimolar amount (0.33 g) of $CuCl_2 \cdot 2H_2O$ was solubilized in 3 mL of H_2O, added to the ligand solution, and stirred for 1 h. Anal. Calcd for $C_8H_{14}N_3O_5SCuCl$: C, 26.42; H, 3.85; N, 11.56; S, 8.81%. Found: C, 26.79; H, 3.42; N, 11.19; S, 8.63. IR (KBr disks, cm^{-1}): 3412 (w) H_2O of crystallization; 3217 (m) ν(NH); 2981 (m) ν(CH); 1723 (m) and 1633 (s) ν(C═O); 1593 (w) ν(C═N); 806 (w) ν(C═S). Mp: 168 °C.

Synthesis of $Cu(Allyl\text{-}H_2ct)Cl \cdot H_2O$ (11). A 0.36 g (1.4 mmol) amount of Allyl-H_3ct was dissolved in 10 mL of MeOH. An equimolar amount (0.23 g) of $CuCl_2 \cdot 2H_2O$ was solubilized in 5 mL of MeOH, added to the ligand solution, and stirred for 1 h. Anal. Calcd for $C_9H_{14}N_3O_5SCuCl$: C, 28.77; H, 3.73; N, 11.19; S, 8.53. Found: C, 29.15; H, 3.39; N, 10.68; S, 8.81. IR (KBr disks, cm^{-1}): 3436 (m) H_2O of crystallization; 3215 (m) ν(NH); 2994 (m) and 2928 (m) ν(CH); 1724 (w) and 1637 (s) ν(C═O); 1580 (m) ν(C═N); 819 (w) ν(C═S). Mp: 143 °C.

Synthesis of $Cu(2,4\text{-}Me_2\text{-}Hct)Cl \cdot H_2O$ (12). A 0.05 g (0.2 mmol) amount of 2,4-Me_2-H_2ct was dissolved in 15 mL of H_2O. An equimolar amount (0.035 g) of $CuCl_2 \cdot 2H_2O$ was dissolved in 3 mL of H_2O, added to the ligand solution, and stirred for 1 h. Anal. Calcd for $C_9H_{15}N_3O_5SCuCl$: C, 26.43; H, 4.13; N, 11.56; S, 8.81. Found: C, 26.91; H, 3.87; N, 11.69; S, 8.55. IR (KBr disks, cm^{-1}): 3440 (m) H_2O of crystallization; 3308 (s) ν(NH); 3213 (w), 3114 (w) and 2912 (vw) ν(CH); 1701 (m) and 1616 (s) ν(C═O); 1563 (m) ν(C═N); 819 (w) ν(C═S). Mp: 190 °C.

Synthesis of $Cu(Ph\text{-}H_2ct)Cl$ (13). A 0.22 g (0.7 mmol) amount of Ph-H_3ct was solubilized in 25 mL of MeOH. An equimolar amount (0.12 g) of $CuCl_2 \cdot 2H_2O$ was dissolved in 5 mL of H_2O, added to the ligand solution, and stirred for 1 h. Anal. Calcd for $C_{12}H_{12}N_3O_4SCuCl$: C, 36.61; H, 3.05; N, 10.68; S, 8.13. Found: C, 37.13; H, 3.41; N, 10.32; S, 8.47. IR (KBr disks, cm^{-1}): 3295 (w) ν(NH); 3064 (vw) and 2953 (vw) ν(CH); 1725 (m) and 1599 (m) ν(C═O); 1493 (m) ν(C═N); 755 (w) ν(C═S). Mp: 172 °C.

Synthesis of $Cu(3\text{-}Me\text{-}Ph\text{-}H_2ct)Cl$ (14). A 0.047 g (0.15 mmol) amount of 3-Me-Ph-H_3ct was dissolved in 15 mL of MeOH. An equimolar amount (0.025 g) of $CuCl_2 \cdot 2H_2O$ was dissolved in 5 mL of H_2O, added to the ligand solution, and stirred for 1 h. Anal. Calcd for $C_{13}H_{15}N_3O_4SCuCl$: C, 38.29; H, 3.68; N, 10.31; S, 7.85. Found: C, 38.45; H, 3.51; N, 10.03; S, 8.15. IR (KBr disks, cm^{-1}): 3418 (w) ν(NH); 3011 (vw) and 2945 (vw) ν(CH); 1719 (m) and 1610 (s) ν(C═O); 1557 (s) ν(C═N); 1492 (s) δ(OH); 1365 (s) δ(CH); 778 (m) ν(C═S). Mp: 180 °C.

Crystallography. Crystal data and details of structure refinements are given in Table 1. All intensity data were collected at room temperature on a Philips diffractometer with Mo Kα radiation (λ = 0.71069 Å) for ligand **3** and complex **9**, while for ligand **1** the intensity data were carried out on an Enraf-Nonius CAD-4 instrument using graphite-monochromatized Cu Kα radiation (λ = 1.54184 Å). The intensities were measured following a modified version[20] of the method of profile analysis by Lehmann and Larsen[21] and were corrected for Lorentz and polarization effects. Calculations

(20) Belletti, D.; Cantoni, A.; Pasquinelli, G. *Gestione on line di diffrattometro a cristallo singolo Siemens AED con sistema IBM PS 2/30*; Internal Report 1/88; Centro di studio per la Strutturistica diffrattometrica del CNR, 1988.

(21) Lehman, M. S.; Larsen, F. K. *Acta Crystallogr. Sect. A* **1974**, *30*, 580−585.

were performed using the WinGX 1.64 program.[22] The structure for all compounds was solved by direct methods using SIR92[23] for ligand **1** and SIR97[24] for the other compounds. Successive Fourier syntheses allowed the assignment of the atoms to the electron density peaks.

For compounds **1**, **3**, and **9** refinements were carried out by full-matrix least-squares cycles (SHELXL-97[25]). Anisotropic thermal parameters were used for non-hydrogen atoms except in ligand **3** for the carbon atoms of the allyl substituent on the aminic nitrogen which present a certain degree of disorder and in complex **9** for a crystallization water molecule O3W that is distributed on two positions (O3W1 and O3W2). For ligand **1** the hydrogen atoms were located on a difference map, except those of the water molecules O5 and O5A, which lie on a symmetry center, and those of the carboxylic groups. In compound **3** all hydrogen atoms of the aliphatic chain, except those of disordered allyl group, are placed in calculated positions. Only the hydrogen atoms of methylene carbon C7 and those of two hydroxylic oxygen were located on a difference map and refined. In complex **9** only the hydrogen atoms of coordinated water molecule were located on a difference map and isotropically refined. All ligand hydrogen atoms were placed in calculated positions and not refined.

Analytical expressions of neutral atom scattering factors were employed according to ref 26. Molecular geometry calculations were performed using the PARST[27] computer program and the structure drawings obtained with the ORTEPIII[28] and PLATON[29] programs.

DNA Interaction Studies. DNA samples were dissolved in aqueous solution 50 mM NaCl, 5 mM Tris, pH 7.2. A solution of CT-DNA (ca. 10^{-5} M in base pair, [bp]) was prepared, and in this buffer it gave a UV absorbance ratio at 260 and 280 nm (A_{260}/A_{280}) of ca. 1.8, indicating that the CT-DNA was sufficiently protein free. The concentration of the nucleic acid solutions was determined by UV absorbance at 260 nm after 1:100 dilution. The extinction coefficient ϵ_{260} was taken as 13 100 M^{-1} cm^{-1} as reported in the literature.[30] Stock solutions were stored at 4 °C and used after no more than 4 days. Binding constants for the interaction of the compounds with the nucleic acid were determined as already described.[31] The intrinsic binding constant K_b for the interaction of the compounds with CT-DNA has been calculated by an absorption spectral titration data using the equation $1/\Delta\epsilon_{ap} = 1/(\Delta\epsilon K_b D) + 1/\Delta\epsilon$, where $\Delta\epsilon_{ap} = |\epsilon_A - \epsilon_F|$, $\Delta\epsilon = |\epsilon_B - \epsilon_F|$, $D =$ [DNA], and ϵ_A , ϵ_B, and ϵ_F are respectively the apparent, bound, and free extinctions coefficient of the compound. K_b is given by the ratio of the slope to intercept when it is reported in plot [DNA]/($\epsilon_A - \epsilon_F$) vs [DNA] and is expressed as M^{-1}. The above-mentioned equation, originally used to calculate the binding constants for hydrophobic derivatives, is now broadly used to investigate a wide variety of metal complexes containing phenanthroline and its derivatives and is usually adopted to obtain binding constants values from metal complexes with different ligands.[14,32,33] Fixed amounts of the ligands and of the complexes were dissolved in CH_3OH because the high solubility of the compounds in this solvent allows one to prepare concentrated solutions and therefore to utilize reduced volumes (5 μL) for titrations. It was also verified that the CH_3OH percentage (0.7%) added to the DNA solution did not interfere with the nucleic acid; in fact the 260 nm absorption band is not subject to modifications in intensity and position. Concentrated solutions of NaCl, Tris-HCl (pH 7.2) buffer, and DNA were prepared. Calculated amounts of the above-mentioned stock solutions were brought to final concentration values of 50 mM NaCl, 5 mM Tris-HCl, and increasing amounts of DNA over a range of DNA concentrations from 10^{-5} to 10^{-3} M and were added to the 5 μL solution of the considered compound to maintain the final volume of the solutions fixed at 700 μL. The compounds were titrated at room temperature. The changes in absorbance of DNA of an intra ligand (IL) band upon each addition were monitored at the maximum wavelengths 284, 281, 288, 290, 290, and 320 nm for **1**, **2**, **6**, **8**, **10**, and **13**, respectively. For compound **10** the titration was monitored also at 629 nm, where the metal d−d transition was observed. The titrations were carried out for a bp/mol ratio r in the range 0.01−8. Melting measurements were carried out in the above-mentioned solutions. DNA (45 μM) was then treated with our compounds at a mol/bp ratio of $r = 0.01$, and each sample was incubated for 24 h at room temperature. Samples were continuously heated with 1° min^{-1} rate of temperature increase while monitoring the absorbance change at 260 nm. The investigated interval of temperature ranged from 50 to 90 °C. Upon reaching 90 °C, samples were cooled back to 50 °C to allow the renaturation process. Values for the melting temperature (T_m) and for the melting interval (ΔT) were determined according to the reported procedures.[34] Differential melting curves were obtained by numerical differentiation of experimental melting curves.

Nuclease Activity: Materials and Method. The DNA cleavage was carried out on double stranded plasmid DNA pBR 322 by electrophoresis. Buffers were prepared using sterile distilled water. Solutions composed by 1.6 μL of plasmid (40 μg/mL), 4 μL of studied compound dissolved in DMSO (0.1 mM), and 8.4 μL Tris buffer solution (10 mM) were incubated for 1 h at 37 °C. This was followed by addition of gel loading solution, and each sample was loaded directly into different wells on a 1.5% agarose gel for analysis by electrophoresis at 75 V for 3 h. The gel was stained with ethidium bromide and photographed under UV light in a transilluminator.

Biological Data: Materials and Methods. The compounds were evaluated for their possible biological activity in DMSO solutions. Different concentration ranges for each of the compounds had to be used because they present different degrees of solubility. At the same time for each experiment the biological effect of DMSO, used as a blank, was determined for each concentration.

Human leukemic cell line U937 from a patient with histiocytic lymphoma has been used. This line was grown in RPMI-1640

(22) Farrugia, L. J. WinGX 1.64. *J. Appl. Crystallogr.* **1999**, *A 32*, 837−838.
(23) Altomare, A.; Cascarano, G.; Giacovazzo, C.; Guagliardi, A. SIR 92. *J. Appl. Crystallogr.* **1993**, *26*, 343−350.
(24) Altomare, A.; Burla, M. C.; Camalli, M.; Cascarano, G.; Giacovazzo, C.; Guagliardi, A.; Moliterni, A. G. G.; Polidori, G.; Spagna, R. SIR 97. *J. Appl. Crystallogr.* **1999**, *32*, 115−122.
(25) Sheldrick, G. *SHELXL 97 A Program for Structure Refinement*; University of Goettingen: Goettingen, Germany, 1997.
(26) *International Tables for X-ray Crystallography*, 4th ed.; Kynoch Press: Birmingham, U.K., 1974.
(27) Nardelli, M. PARST95. An update to PARST: a system of Fortran routines for calculating molecular structure parameters from the results of crystal structure analyses. *J. Appl. Crystallogr.* **1995**, *28*, 659.
(28) Johnson, C. K.; Burnett, M. N. *ORTEPIII*; Report ORNL-6895; Oak Ridge National Laboratory: Oak Ridge, TN, 1996.
(29) Spek, A. L. *PLATON. A Multipurpose Crystallographic Tool*; Utrecht University: Utrecht, The Netherlands, 1999.
(30) Reichmann, M. E.; Rice, S. A.; Thomas, C. A.; Doty, P. *J. Am. Chem. Soc.* **1954**, *76*, 3047−3051.
(31) Wolfe, A.; Shimer, G. H., Jr.; Meehan, T. *Biochem.* **1987**, *26*, 6392−6396.
(32) Liu, J.; Zhang, T.; Lu, T.; Qu, L.; Zhou, H.; Zhang, Q.; Ji, L. *J. Inorg. Biochem.* **2002**, *91*, 269−276.
(33) Mudasir; Yoshioka, N.; Inoue, H. *J. Inorg. Biochem.* **1999**, *77*, 239−247.
(34) Messori, L.; Casini, A.; Vullo, D.; Haroutiunian, S. G.; Dalian, E. B.; Orioli, P. *Inorg. Chim. Acta* **2000**, *303*, 283−286.

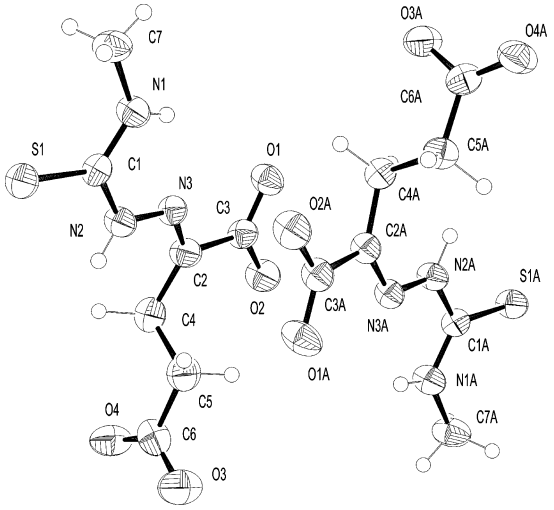

Figure 1. ORTEP drawing of two independent molecules of ligand **1**.

medium added with antibiotics (penicillin 100 U/mL, streptomycin 100 μg/mL), 200 mM L-glutamine, and 10% fetal bovine serum (FBS) and kept at 37 °C in humid atmosphere at 5% CO_2.

Cell Growth. The cells were seeded in a 96-well tray at a concentration of 2×10^5/mL in culture medium and treated with the different compounds. The effect on the cell proliferation process has been determined for each compound to establish the maximum concentration that can be used without appreciable toxic effects. The ranges of the concentrations used were 10−100 μg/mL for compounds **1** and **2** and 5−40 μg/mL for **8**−**10**. Cell mortality, evaluated on the fourth day by the trypan blue exclusion method and determined by using a hemocytometer, never exceeded 5%.

Cells-Cycle Analysis. Cells seeded at 2×10^5/mL exposed to various compounds were analyzed after 24, 48, and 72 h, were washed three times with PBS, and were resuspended in 1 mL of propidium iodide (PI) staining solution (50 μg/mL PI, 100 U/mL RNase, 0.1% Igepal CA-630 in 0.1% sodium citrate) at RT (room temperature) for 45 min in the dark. The cells were acquired on a FACSCalibur flow cytometer (Becton Dickinson, San Jose, CA), and the cell-cycle distribution was analyzed using Flow-Jo software.

Apoptosis Assay. The cell lines were seeded at 8×10^5 mL^{-1} in the presence of the above-mentioned compounds and employed in the apoptosis assay using the agarose gel 2% electrophoresis. To these cells (2×10^6) (washed with PBS at 2000 rpm for 10 min at 4 °C) was added 20 μL of a solution of 10 μM EDTA, 50 mM Tris HCl at pH 8.0, and 0.5% (w/v) sodium laurylsarkosinate. The pellet was subsequently redissolved and added of 2.5 μL of Proteinase K (4 mg/mL) to a final concentration of 0.5 μg/mL. After 1 h at 50 °C 2.5 μL of Rnase A (2 mg/mL) was added and then incubated for 1 h at 50 °C. A gel electrophoresis carried out with the whole sample with a voltage of 80 V allowed one to observe the typical apoptotic DNA fragmentation.

Results and Discussion

Crystal and Molecular Structures. In the structure of Me-H_3ct (**1**) two nonequivalent ligand molecules are present, together with two water molecules lying on symmetry centers at $^1/_2$, $-^1/_2$, 0 and 1, $-^1/_2$, 0. In Figure 1 the structure of the two crystallographically independent ligand molecules is reported. The main difference between the two molecules is in the orientation of the $-CH_2CH_2COOH$ chains. This is highlighted by the two different torsion angles: C4−C5−C6−O3 −174.9(4)° and C4A−C5A−C6A−O3A 8.9(5)°.

Table 2. Bond Distances (Å) for Me-H_3ct (**1**)[a] and Allyl-H_3ct (**3**)

	Me-H_3ct (**1**)		
bond	unlabeled	A labeled	Allyl-H_3ct (**3**)
S1−C1	1.680(4)	1.676(4)	1.670(3)
O1−C3	1.260(6)	1.264(6)	1.319(4)
O2−C3	1.253(5)	1.259(5)	1.218(4)
O3−C6	1.275(6)	1.327(4)	1.328(5)
O4−C6	1.238(5)	1.200(5)	1.197(4)
N1−C1	1.327(6)	1.330(6)	1.317(4)
N1−C7	1.459(6)	1.456(6)	1.461(5)
N2−N3	1.356(4)	1.361(4)	1.347(3)
N2−C1	1.363(5)	1.368(5)	1.381(4)
N3−C2	1.283(5)	1.284(5)	1.288(4)
C2−C3	1.512(6)	1.498(5)	1.490(4)
C2−C4	1.525(7)	1.508(6)	1.498(4)
C4−C5	1.512(6)	1.517(6)	1.521(4)
C5−C6	1.521(8)	1.506(7)	1.490(4)
C7−C8			1.460(7)
C8−C9			1.30(2)

[a] In the third column are reported the data relative to the atoms labeled with the letter A.

The oxygen atoms O1 and O1A present a cis conformation with respect to the N3 and N3A atoms, in a similar way as found for the α-ketoglutaric acid thiosemicarbazone.[35] The conformation of the two molecules is mainly determined by the intramolecular hydrogen bonds N1−H···N3 and N1A−H···N3A, but also C−H···O interactions are present that differ from one molecule to the other, involving respectively the C5 and C4A carbon atoms (C5−H···O1A = 3.390(5) Å, C4A−H···O1 = 3.206(4) Å) as a consequence of the different orientation of the two terminal $-CH_2CH_2COOH$ chains.

The orientation of these two groups is defined by the torsion angles respectively for the two molecules as follows: C2−C4−C5−C6 −176.7(4)° (−antiperiplanar) and C2A−C4A−C5A−C6A 175.3(3)° (antiperiplanar); C4−C5−C6−O3 −174.9(4)° (−antiperiplanar) and C4A−C5A−C6A−O3A 8.9(5)° (synperiplanar); C3−C2−C4−C5 84.4(5)° (synclinal) and C3A−C2A−C4A−C5A 87.5(4)° (synclinal). The molecule is not planar, but the angles between the normal to the planes of the thiourea group and that of the carboxyl group next to the hydrazine nitrogen are fairly small: 3.3(1) and 9.4(1)°, respectively, for the two independent molecules. The plane of the terminal carboxylic group is nearly perpendicular to the mean plane of the remaining side of the molecule (the dihedral angles formed with the thiourea plane are 85.5(1) and 81.1(1)°, respectively, for the two molecules). A major distortion is observed in the hydrazinic chain C1−N2−N3−C2, while in the other molecule the same chain is planar. A comparison between the bond distances in the two molecules shows that they are quite similar, both presenting the thiosemicarbazonic chain in the thionic form (Table 2) as previously found in the α-ketoglutaric acid thiosemicarbazone.[32] The only remarkable difference concerns the carboxylic group of the C6A carbon atom, which shows the distances C6A−O4A (carbonylic) = 1.200(5) Å and C6A−O3A (hydroxylic) = 1.327(4) Å typical of localized bonds, as already noticed for both carboxylic groups of H_3ct,[35] while in the other three

(35) Slouka, J. *Pharmazie* **1960**, *15*, 317−319.

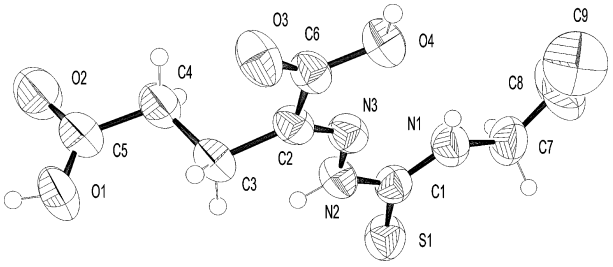

Figure 2. ORTEP drawing of ligand **3**.

Chart 2

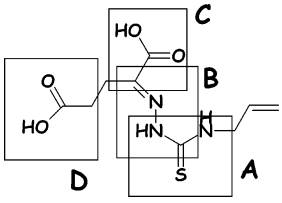

functional groups the C−O distances are delocalized (Table 2). The packing is determined, besides the interactions between the two independent molecules, by an extended network of hydrogen bonds between the two water molecules, the carboxylic groups, and the aminic nitrogen atom. The ribbons so formed develop along the *x* axis at 0 and $^1/_2$ of *z*. These ribbons are then joined along the *y* axis direction by bonds O2···O2A ($x, y + 1, z$) particularly short (2.672(4) Å) and form sheets parallel to the (001) plane linked by the hydrogen bonds N2−H···O4 ($3/2 - x, y - {}^1/_2, -{}^1/_2 - z$) = 3.099(6) Å and N2A−H···O4A ($3/2 - x, y + {}^1/_2, {}^1/_2 - z$) = 2.928(5) Å. The distance O2···O2A is very short probably because of the presence of a strong hydrogen bond even though hydrogen atoms were not experimentally located for the wide delocalization in the two carboxylic groups.

An ORTEP plot of ligand **3** is shown in Figure 2. The molecule is formed by three fragments: the α-ketoglutaric moiety; the thiosemicarbazone chain; the allylic group. The molecular core composed of the thiosemicarbazonic chain and the carboxylic group next to the imine nitrogen is almost planar and the planes A, B, and C (see Chart 2) form dihedral angles of 4.0(2) and 7.1(1)° between them.

This planar conformation is determined by a strong intramolecular hydrogen bond between the aminic nitrogen atom N1 and the imine N3 (N1−H···N3 = 2.594(3) Å). The plane of terminal carboxylic group (D) is nearly perpendicular to the core of the molecule forming an angle of 87.2(1)° with the mean plane as found in ligand **1**. The relative orientation of two carboxylic groups allows hydrogen bonds partly responsible for the molecular packing in the structure.

The orientation of the terminal $-CH_2CH_2COOH$ chain with respect to the remaining side of the molecule is defined by the torsion angles C2−C4−C5−C6 −175.0(2)° (−antiperiplanar) and C4−C5−C6−O3 −173.5(3)° (−antiperiplanar). A comparison of the bond distances with those of ligand **1** and those of the unsubstituted H_3ct[35] shows that also this ligand, **3**, is in the thione form (Table 2); in both carboxylic groups the C−O distances are very different from each other as observed in H_3ct. The allyl groups face one another and

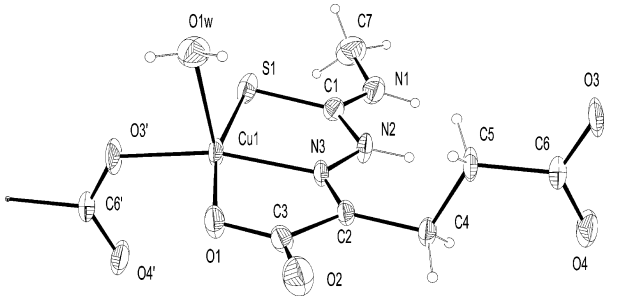

Figure 3. Polymeric chain of coordination polyhedra $[Cu(Me\text{-}Hct)(OH_2)]_n$ in complex **9**.

Table 3. Bond Distances for $[Cu(Me\text{-}Hct)(OH_2)]_n \cdot 2nH_2O$ (**9**)

Cu1−S1	2.305(2)	C5−C6	1.508(8)
Cu1−O1	1.994(5)	O4−C6	1.240(6)
Cu1−O1W	2.306(4)	O1−C3	1.276(8)
Cu1−N3	1.964(4)	O2−C3	1.232(9)
Cu−O3(I)	1.920(3)	O3−C6	1.265(6)
S1−C1	1.713(6)	N1−C1	1.317(6)
N2−N3	1.365(5)	N1−C7	1.453(10)
N2−C1	1.360(9)	C2−C3	1.521(6)
N3−C2	1.285(8)	C4−C5	1.528(6)

are arranged in cavities allowing them to rotate around the simple C−C bond and result statistically distributed in four positions, a feature frequently found in compounds containing the allyl fragment.

In complex **9** the copper atom shows a 4 + 1 pyramidal coordination with the apical position occupied by a water oxygen and the ligand behaving as a SNO tridentate in the basal plane. The fourth basal position is occupied by an O3 carboxylate oxygen of an adjacent molecule translated along the *x* axis, and polymeric chains are thus formed (Figure 3). The ligand is doubly deprotonated and acts as a bridge through a carboxylic group between two copper centers. The basal plane shows a tetrahedral distortion, and the copper atom lies 0.14 Å out of the mean plane toward the O1W atom. The axial bond Cu−O1W is nearly perpendicular to the basal plane [angle formed with the normal to the plane is 9.2(1)°]. The coordination geometry around the copper atom can be described using the angular structural parameter τ,[36] and its value of 0.0065 allows us to confirm a square-pyramidal arrangement.

The ligand is planar in the portion involved in metal coordination, while the terminal chain with the second carboxylic group, which bridges the adjacent molecule, is rotated of 78.8(6)° as in the corresponding free ligand **1**. The Cu−S1−C1−N2−N3 chelation ring presents a ϕ_2 of −161(4)° corresponding to a twist-envelope conformation, while the Cu−N3−C2−C3−O1 is characterized by a ϕ_2 of −26(3)°, i.e., showing a twist conformation.[37]

The Cu−S and Cu−N coordination distances (Table 3) conform to the values found in the literature and also Cu−O1W (apical). The difference between the Cu−O (carboxylate) bond lengths could be ascribed to the constraints determined by the chelation effect.

(36) Addison, A. W.; Rao, T. N.; Reedijk, J.; van Rijn, J.; Verschoor, G. C. *J. Chem. Soc., Dalton Trans.* **1984**, 1349−1355.
(37) Cremer, D.; Pople, J. A. *J. Am. Chem. Soc.* **1975**, *97*, 1354.

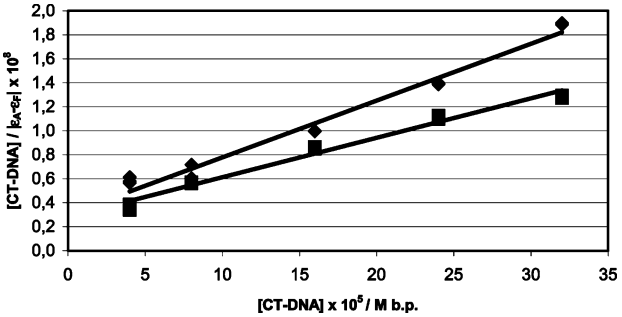

Figure 4. Plot of [CT-DNA]/($\epsilon_A - \epsilon_F$) vs [CT-DNA] for absorption titration with CT-DNA in 50 mM NaCl, 5 mM Tris buffer, pH 7.2 at 25 °C: ◆, **2**; ■, **10**.

Hydrogen bonds between the apical O1W and the carbonylic O2 of the centrosymmetry-related molecule induce the formation of a double polymeric chain of metal complexes which are kept together by two crystallization water molecules.

Absorption Spectral Features of DNA Binding and Thermal Denaturation. To evaluate the behavior of these compounds toward DNA we chose among the ligands Me-H_3ct (**1**) and Ph-H_3ct (**6**) (since they show the largest difference in polarity and sterical hindrance of the substituents) to evaluate if these variables were effective in influencing DNA−compound interactions. Among the complexes, [Cu(Me-H_2ct)Cl]·H_2O (**8**) and Cu(Ph-H_2ct)Cl (**13**) were chosen to study if the presence of the metal interferes with the processes leading to the binding to the nucleic acid in comparison to their parent free ligands. Also [Cu(Et-H_2ct)Cl]·H_2O (**10**), with the ethyl-substituted ligand, was taken into account because from our biological assays this compound resulted to be the most active as regards proliferation inhibition and was therefore subsequently included in the DNA interaction studies together with its free ligand Et-H_3ct (**2**).

The binding constants obtained for ligands **1**, **2**, and **6** were $(1.4 \pm 4) \times 10^3$, $(1.6 \pm 5) \times 10^4$, and $(2.8 \pm 5) \times 10^3$ M^{-1}, respectively. The binding constants for complexes **8**, **10**, and **13** were $(4.5 \pm 5) \times 10^3$, $(2.1 \pm 5) \times 10^4$, and $(9.3 \pm 6) \times 10^3$ M^{-1}, respectively (each experiment was performed in triplicate). As an example, in Figure 4 the plot of [DNA]/($\epsilon_A - \epsilon_F$) vs [DNA] for absorption titration of ligand (**2**) and its copper complex (**10**) is reported, useful to obtain K_b from the ratio of the slope to intercept.

Our experimental K_b values were lower than those observed for classical intercalators (ethidium−DNA, 1.4×10^6 M^{-1} in 25 mM Tris-HCl/40 mM NaCl buffer, pH = 7.9 (ref 38), 3.0×10^6 M^{-1} in 5 mM Tris-HCl/50 mM NaCl buffer, pH = 7.2 (this work)), indicating that the compounds bind DNA with less affinity, as already observed in the literature for copper(II) complexes with macrocyclic ligands[32] and with heterocyclic thiosemicarbazones.[14] Moreover since upon complexation no significant increase of K_b was observed, we can infer that the binding mode to DNA is mainly due to the ligand.

Hypochromism and red shift (bathochromism) in electronic absorption spectra of DNA bound to different compounds is generally assigned to intercalation, involving a strong stacking interaction between the aromatic chromophores and the base pairs of DNA. In this work, for ligands **1**, **2**, and **6** these features were observed with $0 < [DNA]/[ligand] \leq 1$ ratios, while with [DNA]/[ligand] > 1 ratios the bathochromism was conserved but the absorbance values increased as can be observed in Figure 5 (left) where, as an example, is reported the absorption spectra of **1**.

This behavior can be related to the amount of DNA: at the first DNA addition the disappearance of the typical ligand band and the appearance of an absorption band (263 nm) assignable to the DNA−ligand adduct formation are easily observable. At 284 nm, where the compound has its maximum, no absorbance additivity due to the presence of non interacting species was observed. Further DNA additions confirmed this trend.

As regards the examined complexes (**8**, **10**, and **13**) the band of the nonbound complex disappeared probably because of the bathochromism in the same wavelength range covered by the nucleic acid absorbance. This means that these complexes interact with DNA differently from the ligands as can be seen from the different spectroscopic behavior. In Figure 5 (right-hand side) is reported the case of [Cu(Et-H_2ct)Cl]·H_2O (**10**). With the used ratios ($r = 1$, 2, 4, 6, 8), the DNA amount is the major responsible of the absorption in the examined region. To make clear if the absorbance value was due to the compound−DNA interaction and not to DNA alone, the titration was also carried out with lower DNA amounts using the following different ratios: $r = 0.2$, 0.4, 0.6, 0.8, and 1, where [complex] = 40 μM. In this case the DNA absorption did not interfere with the adduct DNA−complex absorption. The obtained K_b value with lower r does not differ significantly from that obtained with higher r, and this confirms our hypothesis (Figure 6).

To further confirm that the added DNA does not interfere with our titration, the experiment was also carried out in the visible region, where only the copper complex absorbs. The ratios used for the experiment were $r = 0.01$, 0.02, 0.05, 0.08, 0.1, and 0.2 and [complex] = 2 mM. The K_b value found was once again the same. This shows that K_b is independent from the chosen absorption band and from the considered concentrations.

The difference with respect to the classical absorption spectral behavior is due to the possibility for our compounds to have many hydrogen-bonding interactions because of the presence of two carboxylic groups and NH functions, in agreement with refs 32 and 14; in addition, the electronic spectra of the adduct with DNA suggests the presence of a new molecular species responsible for the interactions.

K_b values and spectral behavior observed for these compounds are usually found when aspecific interactions with DNA are present,[14,39] but these data do not exclude an intercalative behavior.

(38) Le Pecq, J. B.; Paoletti, C. *J. Mol. Biol.* **1967**, *27*, 87−106.

(39) Pasternack, R. F.; Gibbs, E. J.; Villafranca, J. J. *Biochemistry* **1983**, *22*, 2406−2412.

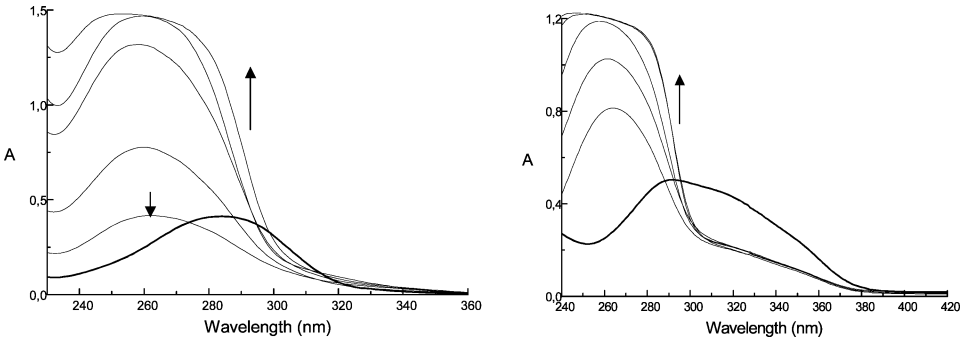

Figure 5. Variation in IL absorption spectra of compounds Me-H_3ct (**1**) (40 μM, left) and [Cu(Et-H_2ct)Cl]·H_2O (**10**) (40 μM, right), with increasing amount of CT-DNA. The ratio r (r = [CT-DNA]/[complex]) varied between 0 (bold line) and 8 in 5 mM Tris-HCl buffer (pH = 7.2), 50 mM NaCl, at 25 °C. The arrows indicate the directions of absorbance changes as a function of r.

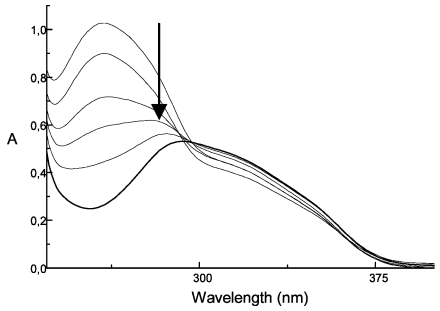

Figure 6. Variation in IL absorption spectra of compounds [Cu(Et-H_2-ct)Cl]·H_2O (**10**) (40 μM), with increasing amount of CT-DNA. The ratio r (r = [CT-DNA]/[complex]) varied between 0 (bold line) and 1 in 5 mM Tris-HCl buffer (pH = 7.2), 50 mM NaCl, at 25 °C. The arrow indicates the directions of absorbance changes as a function of r.

To verify this hypothesis, thermal denaturation profiles of DNA have been studied for compound [Cu(Et-H_2ct)Cl]·H_2O (**10**). The melting temperature (T_m) was compared with that of native CT-DNA T_m (70 °C), and the thermal denaturation profiles and the differential melting curves in the presence of compound [Cu(Et-H_2ct)Cl]·H_2O (**10**) are reported in Figure 7 (left- and right-hand side, respectively).

At the studied concentration, complex [Cu(Et-H_2ct)Cl]·H_2O (**10**), which among these compounds shows the highest K_b and the lowest IC_{50} values, shows a good effect on the melting temperature, suggesting its capability to stabilize the DNA duplex because it significantly increases T_m by 8.5 °C.[34] This experiment confirms the presence of intercalation as one could expect, particularly from square planar copper complexes.

Nuclease Activity. A gel electrophoresis experiment using plasmid pBR322 was performed with all our compounds. At millimolar concentrations all tested compounds appear not to affect pBR322 plasmid (data not shown). Under these experimental conditions there is therefore no production of hydroxyl (OH·) radicals that cleave the sugar phosphate backbone. It can be supposed that our ligands stabilize the higher oxidation state of the copper center, which consequently does not exert its redox activity.

Effects on Cell Proliferation and Cell Cycle Study. From toxicity assays carried out on the tested cell line, the maximum percentage of the DMSO tolerated must not exceed 0.4−0.5%. The effects of both ligands **1** and **2** and of the three complexes **8**−**10** on U937 cell line proliferation on the fourth day are reported in Figure 8. By comparison of the biological effects of our compounds with the cells treated with DMSO alone used as control, ligands **1** and **2** at their maximum reachable concentration in DMSO inhibited cell proliferations of 13% and 30%, respectively, and copper complexes **8** and **9** showed an inhibition activity of 35%, while for complex **10** it reached 50%. Noteworthy is that the complexes exert higher biological activity at lower concentration value with respect to those of the ligands (Figure 8).

Among all the studied compounds, [Cu(Et-H_2ct)Cl]·H_2O (**10**) showed the best activity in inhibiting cell proliferation. For this reason it seemed useful to investigate which phase of the cell cycle was directly implicated in the biological behavior of this complex.

A 48 h treatment on leukemic cell line U937 showed a slow of the cell cycle progression with a 28% reduction of the DNA synthesis phase (phase S) and with an increase of cell population in the G1 and G2/M phases. The percentage distribution of U937 cells in the various phases of the cell cycle is as follows: in the presence of DMSO 0.4% G1 = 46.4%, S = 43.8%, and G2 = 10.4%, and in the presence of compound [Cu(Et-H_2ct)Cl]·H_2O (**10**) G1 = 53.5%, S = 31.5%, and G2 = 15.4%.

It was also verified that after a 48 h treatment period there is no significant apoptosis induction by [Cu(Et-H_2ct)Cl]·H_2O (**10**).

Conclusions

From the observations reported in this paper a series of conclusions can be drawn both from a chemical and from a biological viewpoint.

Looking at the chemical details, we can point out that, among all the substituents introduced on the aminic nitrogen, the ethyl derivatives showed the largest activity and this had already been observed in other aliphatic thiosemicarbazones.[40] By comparison of the biological activity of these compounds with analogous complexes with the nonsubstituted ligand,[18] it can be highlighted that substituents decrease cell proliferation inhibition, except for the case of [Cu(Et-H_2ct)Cl]·H_2O (**10**) that, on the other hand, follows a different pathway from apoptosis induction. The presence of the

(40) Belicchi Ferrari, M.; Bisceglie, F.; Pelosi, G.; Tarasconi, P.; Albertini, R.; Pinelli, S. *J. Inorg. Biochem.* **2001**, *87*, 137−147.

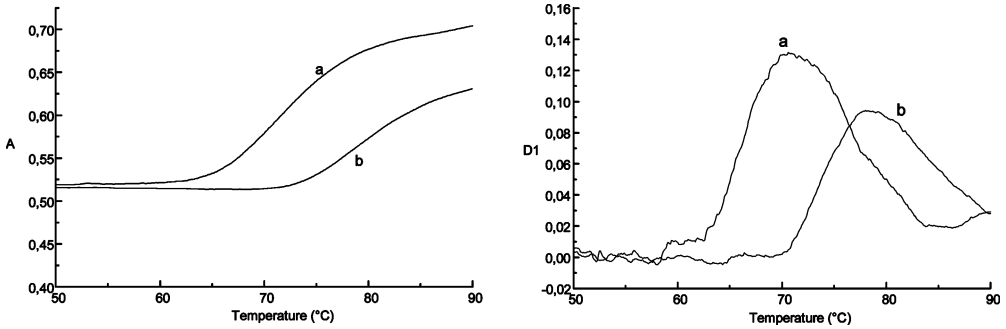

Figure 7. Thermal denaturation profiles (left) and differential melting curves (right) of calf thymus DNA before (a) and after addition of [Cu(Et-H_2ct)Cl]·H_2O (**10**) at $r = 0.01$ (b) where r = [complex]/[DNA]. DNA concentration: 4.5×10^{-5} M. Buffer: 50 mM NaCl, 5 mM Tris-HCl.

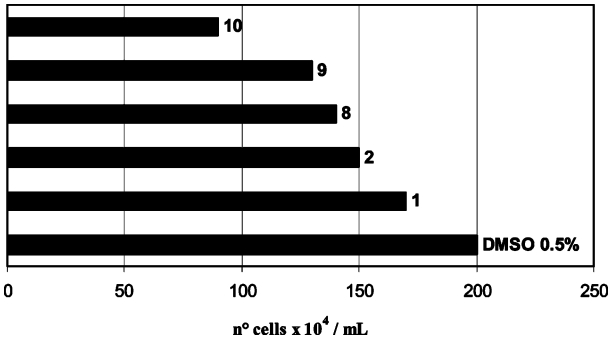

Figure 8. U937 cell proliferation inhibition for compounds **1** (Me-H_3ct; 429 μM), **2** (Et-H_3ct; 377 μM), **8** ([Cu(Me-H_2ct)Cl]·H_2O; 86 μM), **9** ([Cu(Me-Hct)$(OH_2)]_n$·2$n$$H_2O$; 91 μM), and **10** ([Cu(Et-H_2ct)Cl]·H_2O; 24 μM).

thiosemicarbazone free aminic group seems to be determining in inducing apoptosis.[17,18]

Thiosemicarbazones and related molecules have been suggested to act as iron chelators, and their mechanism of action has been assigned to their ability to interfere with DNA synthesis by sequestering iron from ribonucleotide reductase and thus preventing the production of deoxyribonucleotides.[41] If this was the case, we would observe first of all a larger activity of ligands if compared with their metal complexes and moreover an accumulation of cells in phase S because of the impossibility for the cell to cross the damage checkpoint. From the cell cycle analysis we notice instead an accumulation in phase G2 and a depletion of the cells in phase S that is unexpected in the hypothesis of a ribonucleotide reductase inhibition.

Another suggested way of action of these copper compounds is related to their potential capability of generating OH radicals and causing oxidation stress with irreversible damage to DNA with subsequent induction of apoptosis. With our electrophoresis experiments also this mechanism can be excluded since we observe only a tiny amount of nicked plasmid and none in its linear form even with relatively high concentrations of the complexes.

As regards their biological activity, we can therefore conclude that these compounds interfere with the cell cycle at different levels but the mechanisms that lie behind their behavior are still unclear.

Acknowledgment. This work was supported by the Ministero dell'Istruzione Università e Ricerca of Italy (MIUR, cofin. 2001053898).

Supporting Information Available: Crystallographic data in CIF format. This material is available free of charge via the Internet at http://pubs.acs.org.

IC049883B

(41) Richardson, D. R.; Milnes, K. *Blood* **1997**, *89*, 3025−3038.